

Characterization of quantum chaos by the autocorrelation function of spectral determinants

This article has been downloaded from IOPscience. Please scroll down to see the full text article.

1997 J. Phys. A: Math. Gen. 30 3643

(<http://iopscience.iop.org/0305-4470/30/10/035>)

View [the table of contents for this issue](#), or go to the [journal homepage](#) for more

Download details:

IP Address: 171.66.16.71

The article was downloaded on 02/06/2010 at 04:19

Please note that [terms and conditions apply](#).

Characterization of quantum chaos by the autocorrelation function of spectral determinants

S Kettmann†, D Klakow‡ and U Smilansky

Department of Physics of Complex Systems, The Weizmann Institute of Science, Rehovot 76100, Israel

Received 4 November 1996, in final form 18 March 1997

Abstract. The autocorrelation function of spectral determinants is proposed as a convenient tool for the characterization of spectral statistics in general, and for the study of the intimate link between quantum chaos and the random matrix theory, in particular. For this purpose, the correlation functions of spectral determinants are evaluated for various random matrix ensembles, and are compared with the corresponding semiclassical expressions. The method is demonstrated by applying it to the spectra of the quantized Sinai billiards in two and three dimensions.

1. Introduction

One of the most important discoveries in the study of quantum systems which display chaotic dynamics in the classical limit, was the fact that generically, the spectral statistics obey the predictions of random matrix theory (RMT). This observation was originally made on the basis of numerical experiments (see for example [1] for energy spectra, [2] for S -matrix spectra), but during recent years it received a much stronger theoretical foundation [3–7]. The standard tools for the quantitative study of spectral statistics were the n -point correlation functions, or some functions thereof which were usually chosen because of their suitability in the analysis of finite spectral stretches. In the present work we would like to propose a different approach, which is based on the study of the statistical properties of the *spectral determinant*, sometimes referred to as the *secular function*, the *spectral ζ function* or the *characteristic polynomial*: it is the function which vanishes if and only if its argument belongs to the spectrum. The spectral determinant, considered as a function of its variable, is defined in terms of coefficients which can be expressed as functions of the eigenvalues. This is particularly simple for the case of a matrix of finite dimension N , where the characteristic polynomial is defined in terms of its coefficients, which, in turn, can be calculated from the spectrum. Thus, the information stored in the spectral function is equivalent to the information stored in the spectrum, and one may ask why should one study the statistics of the former, when the n -point spectral statistics are so well investigated.

In this paper we shall try to show that in fact the correlation function may offer some important advantages for studying the statistics of the spectrum. To name a few: in general the coefficients in the spectral determinants depend in a complicated way on the spectral

† Present address: Max-Planck Institut für Physik Komplexe Systeme, Außenstelle Stuttgart, 70569 Stuttgart, Germany.

‡ Present address: Institut für Theoretische Physik II, Staudtstrasse 7, Universität Erlangen, 91058 Erlangen, Germany.

points. Sometimes, however, the ensemble averages of these quantities have particularly simple expressions, which are convenient for numerical and theoretical studies. This was the reason why the Essen group [8] studied the statistical properties of the coefficients of the characteristic polynomials for the random circular ensembles. We would like to emphasize other aspects, which are especially important for establishing the connection between quantum chaos and RMT. The Gutzwiller trace formula, which gives the semiclassical theory for the spectral density, typically diverges. The derivation of spectral statistics based on this theory, should therefore be augmented by additional assumptions [3] or *ad hoc* truncation procedures [7]. In contrast, the semiclassical expression for the spectral determinant involves a finite number of periodic orbits, and therefore it converges on the real energy axis. The semiclassical spectral determinant preserves another important property, namely, it is explicitly real for real energies [9–11]. Thus, the semiclassical study of the statistical properties of the spectral determinant can be based on a relatively solid starting point. Last but not least, the semiclassical spectral determinant shares many of its properties with the Riemann Siegel expression for the Riemann ζ function on the critical line. The autocorrelation function for ζ_R is the subject of a study by Keating *et al* [12] which was carried out in parallel to the present work. The rigorous results obtained for the ζ_R case, provide some support to the physically reasonable (yet mathematically uncontrolled) approximations made in the semiclassical theory to be discussed here.

The object we would like to study in the present paper is the autocorrelation function. Denote by $Z(x)$ the secular function, which vanishes at the spectral points $\{x_n\}$. The variable x can stand for the energy, or for the phase variable when the operator under study is a unitary operator such as a S -matrix or a unitary evolution operator. Consider a domain of size Δ centred about x_0 . The autocorrelation function is defined in terms of

$$\bar{C}(\xi; x_0) = \frac{1}{\Delta} \int_{x_0-\Delta/2}^{x_0+\Delta/2} Z(x + \xi/2) Z^*(x - \xi/2) dx. \quad (1)$$

The mean, normalized autocorrelation function is

$$C(\xi) = \frac{\langle \bar{C}(\xi; x_0) \rangle}{\langle \bar{C}(0; x_0) \rangle}. \quad (2)$$

The brackets stand for averaging over an appropriate random matrix ensemble, or for a spectral average which is affected by averaging over x_0 . It is assumed throughout that the correlation variable ξ takes values which are always much smaller than the integration interval Δ .

For a given system, the secular function is uniquely defined up to a multiplicative factor which does not have zeros or poles on the real energy axis. This freedom does not affect the most relevant features of the correlation function which appear on the scale of the mean level spacing.

The behaviour of $C(\xi)$ can be intuitively clarified, by considering two extreme cases: an equally spaced (infinitely rigid) spectrum produces a correlation function which is a strictly periodic function of ξ ,

$$C(\xi) = \cos \pi \xi \quad (3)$$

where ξ is measured in units of the level spacing. On the other hand, a Poissonian spectrum with N spectral points, yields a positive correlation which decays to zero on a scale which is proportional to \sqrt{N} . This can be shown by considering the ensemble of diagonal matrices with independent, Gaussian random diagonal elements with $\langle H_{ii}^2 \rangle = \frac{N^2}{2\pi}$. With this choice,

the average level spacing at $E = 0$ is 1. The correlation function is

$$C_N(\xi) = \left(1 - \frac{\xi^2}{2\pi N^2}\right)^N \rightarrow \exp\left(-\frac{\xi^2}{2\pi N}\right). \tag{4}$$

Thus, the lack of correlation between the energy levels induces a slowly decaying correlation function.

The canonical random ensembles all display level repulsion which induce strong correlations. It is expected, therefore, that the ‘incipient crystalline character’ [13] of the spectrum of these canonical random matrix ensembles will manifest itself by oscillatory, yet slowly decaying, correlation functions. The more rigid the spectrum (larger β), the more marked and persistent the oscillations of $C(\xi)$ will be.

The paper is organized as follows. Section 2 is devoted to the derivation of the autocorrelation function for the standard random matrix ensembles. In section 3, we shall discuss the semiclassical derivation, and compare it with the prediction of RMT. Finally in section 4, we shall present some numerical results which were performed to illustrate and supplement the theoretical derivations.

2. Random matrix theory for the autocorrelation functions

The autocorrelation function takes a particularly simple form in the case of the circular random ensembles. Moreover, the recent results of the Essen group [8] can be directly used to obtain closed expressions for the autocorrelation function. For the sake of completeness, we shall briefly summarize the results for the circular ensembles in the first part of this section. The Gaussian ensembles require some more work: correlation functions of the kind we are interested in were only derived for the unitary (GUE) ensemble [14]. Moreover, the semicircular mean spectral density for the Gaussian ensembles might introduce irrelevant features in the correlation functions if they are not properly treated. The derivation of the autocorrelation function for any Gaussian ensemble which interpolates between the GOE and the GUE will be given in section 4.2 and in the appendix. The effects which are due to the non-uniform mean spectral density are also discussed and are found to be less significant as the dimension of the random matrices increases.

2.1. The circular ensembles

The spectrum of a $N \times N$ unitary matrix S consists of N unimodular eigenvalues $e^{i\theta_l}$, $1 \leq l \leq N$. It is convenient to write the characteristic polynomial such that it is real on the unit circle

$$Z_S(\omega) = e^{\frac{i}{2}(N\omega - \Theta)} \det(I - e^{-i\omega} S) \tag{5}$$

where $e^{i\Theta} = \det(-S)$. The characteristic polynomial can be written as

$$Z_S(\omega) = e^{\frac{i}{2}(N\omega - \Theta)} \sum_{l=0}^N a_l e^{-i\omega l}. \tag{6}$$

The autocorrelation function now reads

$$\bar{C}(\xi) = \frac{1}{2\pi} \int_0^{2\pi} Z_S(\omega + \xi/2) Z_S(\omega - \xi/2) d\omega \tag{7}$$

or explicitly,

$$C_\beta(\xi) = \frac{\sum_{l=0}^N \langle |a_l|^2 \rangle_\beta e^{i\xi(l - \frac{N}{2})}}{\sum_{n=0}^N \langle |a_n|^2 \rangle_\beta} \tag{8}$$

where $\langle \cdot \rangle_\beta$ stands for the average with respect to the spectral measure of the orthogonal ($\beta = 1$), unitary ($\beta = 2$) or symplectic ($\beta = 4$) circular ensembles. The unitarity imposes the identity $|a_n| = |a_{N-n}|$ which guarantees that the autocorrelation function is real, and reduces the effort needed to calculate the ensemble averages.

The ensemble averages $\langle |a_n|^2 \rangle_\beta$ were calculated in [8] for all values of β . We shall quote here the results for the orthogonal and the unitary ensembles:

$$\langle |a_n|^2 \rangle_{\beta=1} = 1 + \frac{n(N-n)}{N+1} \quad \langle |a_n|^2 \rangle_{\beta=2} = 1 \quad \text{for } n = 0 \dots N. \quad (9)$$

It is convenient to introduce the scaled correlation length $\omega = \xi \frac{2\pi}{N}$ and in the limit of large N the sums in (8) can be approximated as integrals, to give

$$C_{\beta=1}(\omega) = \frac{3}{2} \left(\frac{\sin \pi \omega}{\pi \omega} + \frac{1}{\pi^2} \frac{\partial^2}{\partial \omega^2} \frac{\sin \pi \omega}{\pi \omega} \right) \quad C_{\beta=2}(\omega) = \frac{\sin \pi \omega}{\pi \omega}. \quad (10)$$

Equation (10) suggests the following relations between the real correlation functions:

$$C_{\beta=1}(\omega) = -3 \frac{1}{\pi^2 \omega} \frac{\partial}{\partial \omega} C_{\beta=2}(\omega). \quad (11)$$

The two correlation functions are displayed in figure 2. As expected, the more rigid ensemble ($\beta = 2$) shows stronger correlations than the less rigid ensemble.

The expressions derived above for the circular ensembles also appear when the Gaussian ensembles are discussed in the large N limit. A detailed derivation will follow in the next section.

2.2. The Gaussian ensembles

Unlike the circular ensembles, the mean spectral densities for the Gaussian ensembles are not uniform. This has to be incorporated in the definition of the correlation function for the Gaussian ensembles. Otherwise this spurious behaviour may blur the essential correlations. Because of this consideration we shall compute the functions

$$\bar{C}_N(E, \omega) = \left\langle \det \left(E + \frac{\omega}{2} - H \right) \det \left(E - \frac{\omega}{2} - H \right) \right\rangle_H. \quad (12)$$

This function should then be normalized by its value at $\omega = 0$, to obtain the function $C(\omega)$, as defined in equation (2). If we find a dependence of this function on E , even for large N , we will have to perform an integration over a restricted region of the centre $E : |E| \leq \sqrt{N}$. $\langle \cdot \rangle_H$ indicates an average over the ensembles of Hermitian matrices with respect to the measures which will be defined below.

Before doing any calculations, one can gain some insight into this function by writing C_N as

$$\begin{aligned} \bar{C}_N(E, \omega) &= \left\langle \prod_{i=1}^N \left(E - \frac{\omega}{2} - E_i \right) \left(E + \frac{\omega}{2} - E_i \right) \right\rangle_H \\ &= \left\langle \exp \left(\sum_{i=1}^N \left(\ln \left(E - \frac{\omega}{2} - E_i \right) + \ln \left(E + \frac{\omega}{2} - E_i \right) \right) \right) \right\rangle_H. \end{aligned} \quad (13)$$

Hence, C_N can be considered as the partition function of a gas of particles at positions E_i , moving in a quadratic potential (which is provided by the Gaussian measures) and interacting via a logarithmically repulsive interaction with two particles whose positions are fixed at $E + \omega/2$ and $E - \omega/2$ and which do not interact with each other. The interaction between the particles at positions E_i themselves depends on the distribution and the symmetry of the

random Hamiltonian H as we will see in more detail below. It may be useful to come back to this Coulomb gas picture of C_N to understand the results whose derivation we present in the following.

For analytical calculations within an ensemble of random matrices, it is more convenient to write each determinant as the functional integral over two sets of N Grassmann variables, which greatly simplifies the averaging over the weight of the ensemble:

$$\bar{C}_N(E, \omega) = \int d\xi d\xi^* d\eta d\eta^* \langle e^{-\xi^+(E+\frac{\omega}{2}-H)\xi} e^{-\eta^+(E-\frac{\omega}{2}-H)\eta} \rangle_H \quad (14)$$

where $\xi^T = (\xi_1, \dots, \xi_N)$, $\eta^T = (\eta_1, \dots, \eta_N)$, $\xi^+ = (\xi_1^*, \dots, \xi_N^*)$, $\eta^+ = (\eta_1^*, \dots, \eta_N^*)$, and with

$$\int d\xi d\xi^* e^{-\xi^* A \xi} = \det A \quad (15)$$

$$\int d\xi d\xi^* \xi_i^* \xi_j e^{-\xi^* A \xi} = (A^{-1})_{ij} \det A. \quad (16)$$

In this way, the averaging over the Gaussian distributed random matrices H is reduced to a simple Gaussian integral. The remaining Grassmann integrals can be computed to give $C_N(E, \omega)$ as an $(N/2)$ th-order polynomial in ω^2 . Even though we succeeded to do this for arbitrary N , the resulting expressions are rather cumbersome, and since in any case the limit $N \rightarrow \infty$ is of prime interest, we prefer to perform the integrations in the saddle-point approximation which coincides with the exact result for $N \rightarrow \infty$.

We shall treat the unitary and the orthogonal Gaussian random ensembles (and any interpolating ensemble) in a unified way. This is done by writing the Hamiltonian as [15]

$$H = H_s + i\alpha H_a \quad (17)$$

where H_s is a symmetric real matrix, its matrix elements $H_{sij} = H_{sji}$ are real numbers $\forall i, j = 1, \dots, N$. The matrix elements of H_a are asymmetric, $H_{aij} = -H_{aji}$ and real numbers $\forall i \neq j = 1, \dots, N$, since the Hamiltonian H has to be Hermitian.

The random matrices are distributed with a Gaussian measure,

$$\exp(-c\text{Tr}(H^2))dH = \exp\left(-c \sum_{i=1}^N H_{si}^2 - 2c \sum_{i>j} H_{sij}^2 - 2c\alpha^2 \sum_{i>j} H_{aij}^2\right) dH \quad (18)$$

where $c = \pi^2/(4N)$ corresponds to a spectrum with mean level spacing set equal to $d = 1$.

Note that, $\alpha = 0$ corresponds to GOE where there is time reversal symmetry, the Hamiltonian H is symmetric and the distribution is invariant under orthogonal transformations $H \rightarrow OHO^{-1}$. $\alpha = 1$ describes the pure GUE where the time reversal symmetry is broken completely and the Hamiltonian is Hermitian and invariant under unitary transformations $H \rightarrow UHU^{-1}$.

Calculating the correlation function for α between 0 and 1, we obtain the crossover between GOE and GUE.

After performing the Gaussian average over the random matrices (14) reads

$$\begin{aligned} \bar{C}_N(E, \omega) &= \int d\xi d\xi^* d\eta d\eta^* \exp\left(i \sum_{i=1}^N \xi_i^+ \left(E + \frac{\omega}{2}\right) \xi_i + i \sum_{i=1}^N \eta_i^+ \left(E - \frac{\omega}{2}\right) \eta_i\right) \\ &\times \exp\left(-\frac{1}{4c} \sum_{i=1}^N (\xi_i^* \xi_i + \eta_i^* \eta_i)^2\right) \\ &\times \exp\left(-\frac{1}{8c} \sum_{i>j} (\xi_i^* \xi_j + \xi_j^* \xi_i + \eta_i^* \eta_j + \eta_j^* \eta_i)^2\right) \end{aligned}$$

$$\times \exp\left(\alpha^2 \frac{1}{8c} \sum_{i>j} (\xi_i^* \xi_j - \xi_j^* \xi_i + \eta_i^* \eta_j - \eta_j^* \eta_i)^2\right). \quad (19)$$

Thus, we obtain an interacting field theory with interaction strength $1/(4c)$. The Grassmannian functional integration (in the $N \rightarrow \infty$ limit) is described in some detail in the appendix. The resulting normalized correlation function reads

$$C_N(E, \omega) = C_N(\omega) = \int_0^1 d\lambda \lambda \frac{\sin(\pi\omega\lambda)}{\omega} \exp(t^2(\lambda^2 - 1))/C_0(t^2) \quad (20)$$

where the normalization constant is given by

$$C_0(t^2) = \frac{2}{\pi} \int_0^1 d\lambda \lambda^2 \exp(t^2(\lambda^2 - 1)) \quad (21)$$

and $t^2 = 4N\alpha^2$.

The integrals can be evaluated analytically for arbitrary α , giving

$$C_N(\omega) = \frac{\pi^{3/2} \frac{1}{t} \exp\left(\frac{\pi^2 \omega^2}{4t^2}\right) \Im\left[\operatorname{erfc}\left(\frac{\pi\omega}{2t} + it\right)\right] - 2e^{t^2} \frac{\sin(\pi\omega)}{\omega}}{\pi^{3/2} \frac{1}{t} \Im[\operatorname{erfc}(it)] - 2e^{t^2} \pi} \quad (22)$$

where $\operatorname{erfc}(z)$ is the complementary error function.

For further use we study the pure GUE and GOE cases explicitly. The simplest case is for the GUE ensemble ($\alpha = 1$). For large N , the exponential factor in integrand (20) is finite only for $\lambda = 1$, and we obtain:

$$C_N(\omega) = \sin(\pi\omega)/(\pi\omega). \quad (23)$$

For the GOE ensemble ($\alpha = 0$), we find:

$$C_N(\omega) = \frac{3}{\pi} \int_0^1 d\lambda \lambda \frac{\sin(\pi\omega\lambda)}{\omega} = -\frac{6}{\pi^2 \omega} \partial_\omega \frac{\sin(\pi\omega)}{\pi\omega}. \quad (24)$$

It is interesting to note that this coincides also with

$$\frac{3}{2} \int_{-1}^1 d\lambda (1 - \lambda^2) \exp(i\omega\lambda) \quad (25)$$

which coincides with Efetov's result for the pure GOE ensemble.

3. Semiclassical theory

The semiclassical quantization scheme, which is to be used in the following, is the scattering approach [10], (see also [9]) in which one defines a semiclassical *unitary* $S(E)$ operator of dimension Λ and the secular equation, defined to be real for real energies, can be written as

$$Z(E) = e^{-i\Theta(E)/2} \det(I - S(E)) \quad (26)$$

where $\Theta(E)$ is the total phase shift:

$$e^{i\Theta(E)} = \det(-S(E)). \quad (27)$$

It is assumed that the classical analogue of S is an area preserving map \mathcal{M} acting on a Poincaré section with a phase space area A . In the semiclassical limit, Λ is the integer part of $A/2\pi\hbar$. In the same limit, the total phase is related to the smooth spectral counting function

$$\Theta(E) \approx 2\pi \bar{N}(E). \quad (28)$$

The secular equation is real by construction. It can also be expressed in terms of the eigenphases $\theta_l(E)$ of $S(E)$, or as the characteristic polynomial of $S(E)$ evaluated at $z = 1$:

$$Z(E) = e^{-i\Theta(E)/2} \left[\prod_{l=1}^{\Lambda} (1 - ze^{i\theta_l(E)}) \right]_{z=1} = e^{-i\Theta(E)/2} \left[\sum_{l=0}^{\Lambda} a_l(E) z^l \right]_{z=1}. \tag{29}$$

The unitarity of $S(E)$ leads to the relations

$$e^{-i\Theta/2} a_l = e^{i\Theta/2} a_{\Lambda-l}^* \tag{30}$$

which can be used to rewrite (29) as

$$Z(E) = e^{-i\Theta(E)/2} \sum_{l=0}^{[\Lambda/2]} a_l(E) + \text{cc}. \tag{31}$$

To calculate the correlation function, we remember that the a_l are the fully symmetric, homogeneous polynomials in the $e^{i\theta_m}$ of the order of l . We can approximate their variation with energy by writing

$$a_l(E + \epsilon/2) \approx a_l(E) e^{i\tau\epsilon/2} \tag{32}$$

where τ is the average value of the partial delay times $\tau_l = \frac{\partial\theta_l(E)}{\partial E}$. The distribution of the τ_l is known to be narrowly centred about the mean value, τ [10]. It follows from (28) that

$$\tau = 2\pi\bar{d}/\Lambda. \tag{33}$$

The autocorrelation function now reads

$$\begin{aligned} \bar{C}(\epsilon) &= \frac{1}{\Delta E} \int_{E_0-\Delta E/2}^{E_0+\Delta E/2} dE \langle Z(E + \epsilon/2) Z(E - \epsilon/2) \rangle \\ &\approx \sum_{l=0}^{\Lambda} \langle |a_l|^2 \rangle_{\Delta E} e^{i\tau\epsilon(\Lambda/2-l)}. \end{aligned} \tag{34}$$

Where we made use of the fact that the interval ΔE is large on the quantum scale so that the phases $\theta_l(E)$ make many revolutions when E traverses the interval ΔE . We may now denote the scaled energy by $\omega = \epsilon\bar{d}$, and use the relation $\tau\epsilon = \frac{2\pi}{\Lambda}\epsilon\bar{d} = \frac{2\pi}{\Lambda}\omega$. The last equation shows that the autocorrelation function $\bar{C}(\epsilon)$ can be also interpreted as the autocorrelation of the secular equation of the ensemble of $S(E)$ matrices averaged over the energy interval ΔE . Hence, when comparing the results of the semiclassical theory with the predictions of RMT, we shall use the RMT expression for the *circular* ensembles (8), even though our starting point was the spectral determinants of the Hamiltonian.

To introduce the semiclassical theory for the autocorrelation function, it is useful to recall some exact relations which enable us to express the coefficients a_l in terms of $\text{tr}S^n$. This is done by iterating the Newton identities

$$a_l = -\frac{1}{l} \left(\text{tr}S^l + \sum_{k=1}^{l-1} a_k \text{tr}S^{l-k} \right). \tag{35}$$

An explicit solution of the Newton identities is given by the *Plemelj–Smithies formula* [21]

$$a_l = \frac{(-1)^l}{l!} \begin{vmatrix} s_1 & s_2 & s_3 & \cdot & \cdot & \cdot & s_l \\ 1 & s_1 & s_2 & \cdot & \cdot & \cdot & s_{l-1} \\ 0 & 2 & s_1 & s_2 & \cdot & \cdot & s_{l-2} \\ 0 & 0 & 3 & s_1 & \cdot & \cdot & s_{l-3} \\ \cdot & \cdot & \cdot & \cdot & \cdot & \cdot & \cdot \\ \cdot & \cdot & \cdot & \cdot & \cdot & \cdot & \cdot \\ 0 & \cdot & \cdot & \cdot & 0 & l-1 & s_1 \end{vmatrix} \tag{36}$$

where we use the notation

$$s_l = \text{tr} S^l. \tag{37}$$

Result (36) can be easily proved by expanding the determinant with respect to the last column. Writing down the explicit expression of the determinant, one obtains

$$a_l = -\frac{1}{l} \left(s_l + \sum_{\mathbf{l}} \frac{(-1)^n}{\prod_{i=1}^n l_i} s_{l-l_1} s_{l_1-l_2} \dots s_{l_{n-1}-l_n} s_{l_n} \right) \tag{38}$$

where the summation is over all vectors \mathbf{l} with integer entries such that $l > l_1 > l_2 > \dots > l_n \geq 1$. The last equation can also be directly derived from (35) by successive iterations.

The semiclassical approximation is introduced at this point: the S operator is considered as the quantum analogue of the classical evolution operator of the relevant Poincaré map \mathcal{M} . Hence $\text{tr} S^n$ is expressed semiclassically in terms of periodic orbits which traverse the Poincaré section n times.

$$s_n = \text{tr} S^n \approx \sum_p \frac{g_p n_p e^{ir(S_p/\hbar - \nu_p \frac{\pi}{2})}}{|\det(I - M_p^r)|^{\frac{1}{2}}}. \tag{39}$$

The summation is extended over all primitive periodic orbits p of the Poincaré map, with periods n_p which are divisors of n , so that $n = n_p r$. g_p stands for the number of distinct symmetry conjugate orbits, M_p is the monodromy matrix, S_p and ν_p are the action and the Maslov index, respectively.

To obtain the semiclassical expression for the coefficients of the autocorrelation function, we have to substitute the semiclassical expression (39) into (38). When this is done, one obtains the standard *composite orbits* expansion of the spectral determinant [10, 11]. Taking the absolute square and averaging over the energy interval, we make use of the diagonal approximation,

$$\langle s_n s_m^* \rangle_{\Delta E} \approx \delta_{nm} \sum_p \frac{g_p^2 n_p^2}{|\det(I - M_p^r)|} \approx \delta_{nm} \sum_p \frac{g^2 n^2}{|\det(I - M_p)|} \tag{40}$$

which is valid because of the rapid oscillating phases in (39). The right expression in (40) uses the observation that for large n the primitive orbits dominate the periodic orbit sum. Under these conditions, it is allowed to replace g_p by its mean value g . The argument which was used to justify the diagonal approximation for $\langle s_n s_m^* \rangle_{\Delta E}$ can be used for taking the average of the product of any number of s_n factors. Due to the assumed lack of correlations between the phase factors, one finds that the diagonal approximation implies that the s_n form an ensemble of independent random Gaussian variables. This observation is valid as long as repetitions of primitive periodic orbits can be neglected which is a standard element in the semiclassical theory of spectral fluctuations [22]. We shall denote the variances of the s_n distributions by

$$\langle |s_n|^2 \rangle = \langle |s_n|^2 \rangle_{\Delta E} = \sum_p \frac{g^2 n^2}{|\det(I - M_p)|}. \tag{41}$$

The first step in implementing the diagonal approximation for $\langle |a_l|^2 \rangle_{\Delta E}$ is to isolate terms which, upon averaging, do not yield vanishing contributions because of unmatched phase factors. Thus,

$$\begin{aligned} \langle |a_l|^2 \rangle_{\Delta E} = & \frac{1}{l^2} \left[\langle s_l s_l^* \rangle_{\Delta E} + \left\langle \sum_{l_1} \sum_{m_1} \frac{s_{l-l_1} s_{l_1} s_{l-m_1}^* s_{m_1}^*}{l_1 m_1} \right\rangle_{\Delta E} \right. \\ & \left. + \left\langle \sum_{l_1, l_2} \sum_{m_1, m_2} \frac{s_{l-l_1} s_{l_1-l_2} s_{l_2} s_{l-m_1}^* s_{m_1-m_2}^* s_{m_2}^*}{l_1 l_2 m_1 m_2} \right\rangle_{\Delta E} + \dots \right] \tag{42} \end{aligned}$$

where the summations in the n th term are restricted to the domains $l > l_1 > l_2 > \dots > l_n \geq 1$ and $l > m_1 > m_2 > \dots > m_n \geq 1$. The diagonal approximation which is synonymous to treating the s_n as random Gaussian variables enables us to derive the following expression for $\langle |a_l|^2 \rangle_{\Delta E}$

$$\langle |a_l|^2 \rangle_{\Delta E} \approx \frac{1}{l} \left[\frac{\langle |s_l|^2 \rangle}{l} + \sum_{n=1}^{l-1} \sum_{l_1 \dots l_n} \frac{1}{\prod_j l_j} \frac{\langle |s_{l-l_1}|^2 \rangle}{l-l_1} \frac{\langle |s_{l_1-l_2}|^2 \rangle}{l_1-l_2} \dots \frac{\langle |s_{l_n}|^2 \rangle}{l_n} \right] \tag{43}$$

where the summation is carried with the restriction $l > l_1 > \dots > l_n \geq 1$.

At this point it is instructive to consider the Fredholm determinant for the *classical* evolution (Frobenius Peron) operator

$$U(\mathbf{x}, \mathbf{x}') = \delta(\mathbf{x}' - \mathcal{M}(\mathbf{x})) \tag{44}$$

where \mathbf{x} is a point on the classical Poincaré section. A straight forward integration gives

$$u_l = \text{tr} U^l = \sum_p \frac{l_p g_p}{|\det(I - M_p^r)|} \approx \sum_p \frac{l g}{|\det(I - M_p)|} = \frac{1}{g l} \langle |s_l|^2 \rangle. \tag{45}$$

The uniform coverage of phase space by the chaotic trajectories implies that $u_l \approx 1$ for sufficiently large l . In other words,

$$\langle |s_l|^2 \rangle \approx g l \quad \text{for } l > 1 \tag{46}$$

which is the well known Hannay and Ozorio de Almeida sum rule [22]. Using this estimate for all $\langle |s_l|^2 \rangle$ in (43) we find

$$\langle |a_l|^2 \rangle_{\Delta E} \approx \frac{g}{l} \left(1 + \sum_{n=1}^{l-1} g^n \sum_{l > l_1 \dots l_n \geq 1} \frac{1}{\prod_j l_j} \right) = \frac{g}{l} \left(1 + \sum_{n=1}^{l-1} g^n I_n(l) \right) \tag{47}$$

where

$$I_n(l) = \sum_{l_1=n}^{l-1} \frac{1}{l_1} \sum_{l_2=n-1}^{l_1} \frac{1}{l_2} \dots \sum_{l_{n-1}=2}^{l_{n-2}} \frac{1}{l_{n-1}} \sum_{l_n=1}^{l_{n-1}} \frac{1}{l_n}. \tag{48}$$

The lower and upper summation indices follow from the restriction $l > l_1 > \dots > l_n \geq 1$. We now observe that the functions $I_n(l)$ satisfy the recursion relations

$$I_n(l) = -\frac{1}{l} I_{n-1}(l) + \sum_{r=n}^l \frac{1}{r} I_{n-1}(r) \tag{49}$$

which is equivalent to

$$I_n(l) - I_n(l-1) = \frac{1}{l-1} I_{n-1}(l-1) \tag{50}$$

and it is subject to the condition $I_l(l) = I_l(l-1) = 0$. Denote

$$f_l(g) = 1 + \sum_{n=1}^{l-1} g^n I_n(l). \tag{51}$$

Multiplying (50) by g^n and summing over n one obtains

$$f_l(g) = \frac{l-1+g}{l-1} f_{l-1}(g) \quad \text{with } f_1(g) = 1. \tag{52}$$

Hence, for any integer g

$$f_l(g) = \frac{(l-1+g)!}{(l-1)!g!} = \binom{l-1+g}{g}. \tag{53}$$

For the cases of interest here, $f_l(g = 1) = l$ and $f_l(g = 2) = l(l + 1)/2$. These expressions can be substituted into (47) to give

$$\langle |a_l|^2 \rangle_{\Delta E}(g) = \frac{g}{l} f_l(g) = \begin{cases} 1 & \text{for } g = 1 \\ 1 + l & \text{for } g = 2. \end{cases} \quad (54)$$

This is the central result of the present section. It should be augmented by the identity

$$\langle |a_l|^2 \rangle_{\Delta E} = \langle |a_{\Lambda-l}|^2 \rangle_{\Delta E} \quad (55)$$

which is due to unitarity, and then compared with the results of RMT (9).

Systems *without* time reversal symmetry (TRS) have $g = 1$, so that the semiclassical result (54) coincides with the prediction of RMT for the CUE.

In chaotic systems *with* TRS, $g = 2$ and

$$\langle |a_l|^2 \rangle_{\Delta E} \approx \begin{cases} 1 + l & \text{for } 1 < l \leq \Lambda/2 \\ 1 + \Lambda - l & \text{for } \Lambda > l \geq \Lambda/2. \end{cases} \quad (56)$$

This expression does not reproduce the RMT result for the COE case [8]

$$\langle |a_l|^2 \rangle_{\text{COE}} = 1 + l \frac{\Lambda}{\Lambda + 1} - l^2 \frac{1}{\Lambda + 1}. \quad (57)$$

However, for large Λ , where the semiclassical approximation is justified, the semiclassical result reproduces the exact expression in a domain of l values of size $\sqrt{\Lambda}$ in the vicinity of the endpoints of the l interval, $l = 0$ and $l = \Lambda$. The deterioration of the quality of the agreement between the semiclassical and the RMT expressions when TRS is imposed is typical, and it is an enigma in the field of quantum chaos. This is a typical behaviour of the semiclassical approximation, first discussed by Berry [3].

We shall now use the results of the previous sections to investigate the connection between the spectral autocorrelation function and the Ruelle ζ function for the classical mapping \mathcal{M} . The Ruelle ζ is constructed from the Fredholm determinant of the classical evolution (Frobenius Peron) operator by

$$\zeta(s) = (\det(I - e^{-s}U))^{-1} = \sum_{l=0}^{\infty} A_l^{\text{cl}} e^{-sl}. \quad (58)$$

Using the same methods as above, one can easily derive the explicit expression for the coefficients,

$$A_l^{\text{cl}} = \frac{1}{l} \left(u_l + \sum_l \frac{1}{\prod_{i=1}^n l_i} u_{l-l_1} u_{l_1-l_2} \dots u_{l_{n-1}-l_n} u_{l_n} \right) \quad (59)$$

and compare it with the coefficients of the semiclassical correlation function (43) in which the relation $s_l \approx gl u_l$ is used,

$$\langle |a_l|^2 \rangle_{\Delta E} \approx \frac{g}{l} \left(u_l + \sum_l g^n \frac{1}{\prod_{j=1}^n l_j} u_{l-l_1} u_{l_1-l_2} \dots u_{l_{n-1}-l_n} u_{l_n} \right). \quad (60)$$

For systems without TRS $g = 1$, and one obtains

$$\langle |a_l|^2 \rangle_{\Delta E} \approx A_l^{\text{cl}}. \quad (61)$$

This close relationship between the *quantum* autocorrelation function and the *classical* Ruelle ζ function is another manifestation of the observation of [5–7] on the role played by the Ruelle ζ function in the semiclassical theory of spectral correlations. However, one has to be careful and modify this statement by noting that only a *finite* number of coefficients

are used in the spectral autocorrelation function. As a matter of fact, only the first $\Lambda/2$ are used. Those with $\Lambda/2 \leq l \leq \Lambda$ must be defined by (55) due to unitarity, and the rest are set to zero. This is where the (topological) Heisenberg time enters the semiclassical theory. It should be emphasized that the truncation and the symmetry are essential elements, without which the semiclassical theory yields wrong results. Therefore, the identification of $C(w)$ as $\zeta(i\pi w)$ is not allowed.

Systems with TRS have $g = 2$. In this case one can identify the coefficients $\langle |a_l|^2 \rangle_{\Delta E}$ with the coefficients of the function

$$\zeta_g(s) = (\det(I - g e^{-s} U))^{-1} = \sum_{l=0}^{\infty} A_l^{\text{cl}}(g) e^{-sl}. \quad (62)$$

For large s one can use the approximate relation $\zeta_g(s) \approx (\zeta(s))^g$. The fact that $(\zeta(s))^2$ is the classical function which appears in the semiclassical approximation for spectral statistics in systems with TRS was previously discussed in [7]. The remarks made above concerning the relation between the autocorrelation function $C(\omega)$ and the classical function $\zeta_g(s)$ also hold in the present case.

The explicit results obtained above are valid under the condition that the classical orbits uniformly cover phase space, and uniformity is achieved within a short time. Only for such systems $u_n \approx 1$. There are, however, other chaotic systems for which the coverage of phase space is diffusive. Then, u_n can be identified with the *classical return probability*, which for diffusion in d dimensions is proportional to $n^{-d/2}$. One can also work out the spectral autocorrelation function for these systems. This subject will be pursued elsewhere.

4. Numerical results and illustrations

In the previous sections we discussed the average autocorrelation functions of spectral determinants for various random matrix ensembles, and the corresponding semiclassical expressions. Before being able to compare the RMT results with spectral data of quantum chaotic systems, we had to clarify a few practical points. The results for the Gaussian ensembles are obtained in the large- N limit, while all the numerical work can be carried out on spectral intervals of *finite* length. Since the differences between the correlation functions for the different ensembles are not too large, it was important to develop tools to check to what extent the finite- N calculations approach the $N \rightarrow \infty$ limit. For the GOE case, the analytic theory becomes rather cumbersome. The analytic results of [8] for the circular ensembles cannot be used directly for this purpose, because the circular and the Gaussian ensembles are expected to coincide only in the $N \rightarrow \infty$ limit. To check this point, we developed an efficient sampling method based on the metropolis algorithm [18], with which we could calculate the expectation values of any property for any of the matrix ensembles both accurately and efficiently. This was an important tool in our work and we shall describe it in section 4.1.

Spectral determinants of unbounded Hermitian operators do not converge unless properly regularized. In practical applications, one has to make a choice of the regularization method. In section 4.2 we discuss two alternative approaches and show how they are applied to the analysis of long spectral intervals of Sinai billiards in two and in three dimensions.

4.1. The metropolis algorithm for RMT

The metropolis algorithm (MA) generates a *finite* ensemble of spectral sequences which are statistically independent, and which are distributed according to a prescribed probability

distribution. This finite ensemble is used to perform averages which are guaranteed to converge to the exact ensemble averages, when the number of members in the ensemble increases.

The MA for the circular ensembles is defined by the N -point spectral probability distribution

$$p(\boldsymbol{\theta}) = \mathcal{N} \prod_{1 \leq k < l \leq N} |e^{i\theta_k} - e^{i\theta_l}|^\beta \quad (63)$$

where $\boldsymbol{\theta} = \{\theta_1, \dots, \theta_N\}$, $0 \leq \theta_l \leq 2\pi$, and \mathcal{N} is a normalization constant. The MA proceeds as follows. Starting from an initial vector $\boldsymbol{\theta}_n$, a new vector $\boldsymbol{\theta}_{n+1} = \boldsymbol{\theta}_n + \boldsymbol{\Delta}\boldsymbol{\theta}_n$ is determined with the components of $\boldsymbol{\Delta}\boldsymbol{\theta}_n$ randomly chosen from $[-\Delta\theta_{\text{Max}} : \Delta\theta_{\text{Max}}]$.

Denote

$$r = p(\boldsymbol{\theta}_{n+1})/p(\boldsymbol{\theta}_n). \quad (64)$$

A step is accepted if $r > 1$ or $\eta < r$ where $\eta \in [0, 1]$ is a new random number at each step. As the algorithm depends only on the ratio r , the normalization constant is irrelevant. The choice of $\Delta\theta_{\text{Max}}$ is crucial for near optimal performance of the algorithm and we use $\Delta\theta_{\text{Max}} = 0.02$ for $N = 40$ and $\Delta\theta_{\text{Max}} = 0.007$ for $N = 80$. For these parameters, approximately 50% of the metropolis steps are accepted. The initial vector $\boldsymbol{\theta}_0$ is chosen at random and the transients due to the initial choice are erased after a few iterations since the ‘random walker’ $\boldsymbol{\theta}_n$ advances quickly towards the most probable domain. Out of all the vectors $\boldsymbol{\theta}_n$ only a small fraction is accepted to the ensemble in order to obtain an uncorrelated sample. Each run generates a set of 2000 properly distributed vectors which are then used for further analysis. We checked the convergence with respect to the ensemble size, and found that a set of 2000 spectra is sufficiently large to obtain reliable results.

The same algorithm can be used to sample the probability measure of the Gaussian ensembles

$$p(\mathbf{x}) = \mathcal{N} e^{-\frac{\beta}{2} \sum_{i=1}^N x_i^2} \prod_{1 \leq i < j \leq N} |x_i - x_j|^\beta. \quad (65)$$

One has to exercise some care to avoid the choice of initial conditions which have vanishingly small probability due to the exponential term in (65).

As the first application, we studied the difference between the autocorrelation functions for the circular ensembles ($\beta = 1, 2, 4$) and their corresponding Gaussian ensembles for a *finite* dimension $N = 40$. We used definitions (1) and (2) for the autocorrelation functions. For the circular ensemble, the domain of integration is $[0, 2\pi]$ and for the Gaussian ensembles we limited the integration domain to the interval $|E| \leq \sqrt{N}$ to avoid deformations whose origin is the non-uniform semicircular level density. Figure 1 shows small yet systematic differences between the Gaussian and circular ensembles which are most pronounced for the symplectic and the orthogonal ensembles. The differences between the unitary ensembles is the smallest. The overall agreement is rather good, as expected when the limit $N \rightarrow \infty$ is approached.

The same trend persists also when one compares the $N = 40$ cases for the Gaussian ensembles with the expressions derived in section 2 for $N \rightarrow \infty$. This is shown in figure 2. We see again that the $N = 40$ data is fairly close to the infinite limit for the GUE case. In the GOE case the $N = 40$ data is significantly different from the $N \rightarrow \infty$ limit.

We used two independent ways of treating a given large spectrum. In the first method the large spectrum with N_{total} eigenvalues is ‘chopped’ to a number of smaller subintervals. Given a large spectrum, one can chop it in various ways, and one has to find a compromise which provides a sufficiently large ensemble of not too short intervals. We worked with

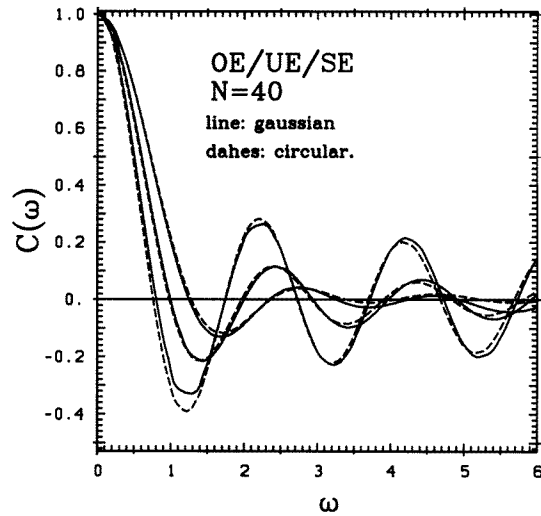


Figure 1. $C(\omega)$ for Gaussian (full curve) and circular (broken curve) ensemble. Results are shown for the orthogonal (most strongly damped) the unitary (middle) and symplectic ensemble (least damped).

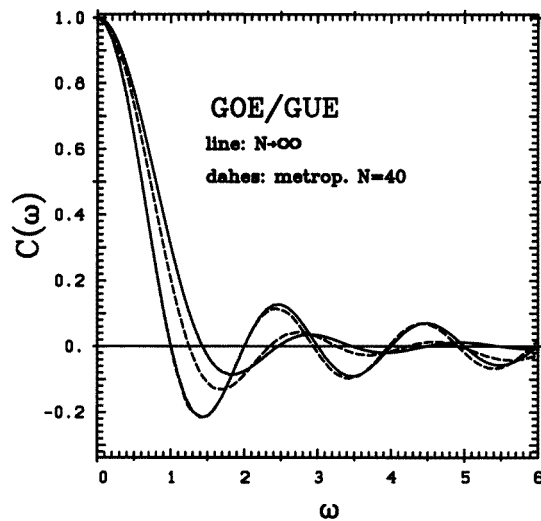


Figure 2. Comparison of $N \rightarrow \infty$ results (full curve) with the $N = 40$ (metropolis) data for the GOE and GUE.

$\approx N_{\text{total}}/40$ subintervals of $N = 40$ eigenvalues. Each subinterval is unfolded to a mean spacing of 1 and is shifted to be centred around $E = 0$. This procedure puts the subintervals on an equal footing. For the calculation of the correlation function, the integration is limited to $|E| < \sqrt{N}$. The ensemble averaged autocorrelation $\bar{C}(\omega)$ is normalized by $\bar{C}(\omega = 0)$. The calculation of the autocorrelation function is similar to the way by which we used the MA samples which were constructed according to the Gaussian measures. An alternative definition would have been to consider the autocorrelation function of the spectral determinant built from the entire large spectrum. Definition (1) will be harder

to apply because both the numerator and the denominator diverge with either $N = N_{\text{total}}$ or E . This difficulty is related to the well known problem of regularization of spectral determinants, the regularization scheme we have chosen is as follows. We shift the origin of the energy axis to the centre of gravity of the large spectrum, and consider the secular function

$$Z_R(E) = \prod_{i=-N}^{N-1} \left(1 - \frac{E}{E_i}\right). \quad (66)$$

This function is defined also in the limit of $N \rightarrow \infty$ as long as the symmetric construction is maintained in the limiting procedure. However, for finite N the function $Z_R(E)$ diverges as E^{2N+1} for sufficiently large E . This can be cured by a regularization factor whose origin can be illustrated by considering the spectral determinant for an equidistant spectrum:

$$p_R(E) = \prod_{i=-N}^{N-1} \left(1 - \frac{E}{i + \frac{1}{2}}\right) = \frac{\Gamma(N + \frac{1}{2} - E)\Gamma(-N + \frac{1}{2})}{\Gamma(-N + \frac{1}{2} - E)\Gamma(N + \frac{1}{2})}. \quad (67)$$

Using the asymptotic expressions for the Γ function one obtains

$$p_R(E) \approx \cos(\pi E) e^{\frac{E^2}{N}}. \quad (68)$$

which is valid for $|E| < E_{\text{max}}(N)$ where $\sqrt{N} < E_{\text{max}}(N) \ll N$. This suggests the definition of a regularized corrected spectral determinant

$$Z_{\tilde{R}}(E) = e^{-\frac{E^2}{N}} \prod_{i=1}^N \left(1 - \frac{E}{E_i}\right). \quad (69)$$

Where the E_i are the unfolded, symmetrically centred spectrum.

The autocorrelation function can now be calculated using

$$\bar{C}_{\tilde{R}}(\omega) = \int_{-\tilde{N}}^{\tilde{N}} Z_{\tilde{R}}\left(E - \frac{\omega}{2}\right) Z_{\tilde{R}}\left(E + \frac{\omega}{2}\right) dE. \quad (70)$$

Note that all eigenvalues are used in one run. Here \tilde{N} is proportional to N , but smaller than $N/2$ as even the regularized spectral determinant is much larger than 1 at the edges of the spectrum. We arbitrarily used $\tilde{N} = N/6$ which yields good results.

As long as N is finite the correlation function based on the regularized polynomial can be expressed as

$$C_R(\omega) = \langle \bar{C}_R(\omega) \rangle = \left\langle \frac{\bar{C}(\omega)}{\bar{C}(0)} \right\rangle. \quad (71)$$

Thus, the difference between the two definitions of the correlation function comes from the different order of the operations of averaging and normalizing. In figure 3, we compare the correlation functions obtained by the two averaging methods. The broken and full curves are MA runs for $N = 40$ with GOE statistics, using the original (2) and regularized (71) definitions, respectively. The regularized correlation function is less damped, and it resembles the non-regularized function for GUE. (The RMT expression for the correlation function (71) for the GUE was considered in [14].)

We have emphasized several times in the discussion above that the expectation value of the autocorrelation function depends on all the n -point spectral statistics, and therefore does not, in principle, contain any new information. However, since a typical spectral analysis is usually carried out in terms of only a few statistical measures, it is worth while to check to what extent the information in the autocorrelation function overlaps with the most common statistics—the nearest-neighbour distribution $P(s)$.

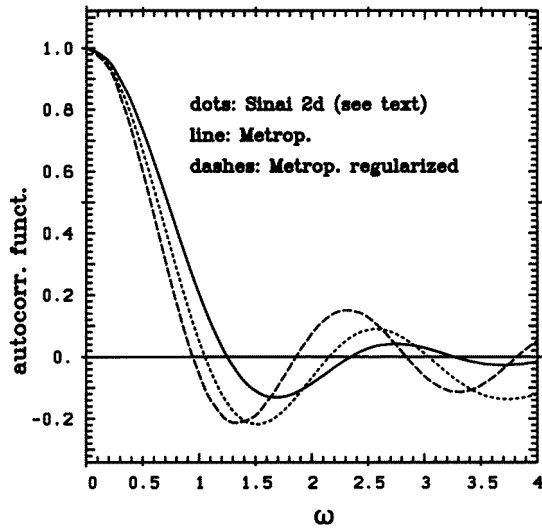


Figure 3. Full curve: autocorrelation function $C(\omega)$ for GOE using metropolis data for $N = 40$; broken curve: same as the previous but regularized $C_R(\omega)$; dotted curve: regularized and corrected $C_{\bar{R}}(\omega)$ for the two-dimensional Sinai billiard.

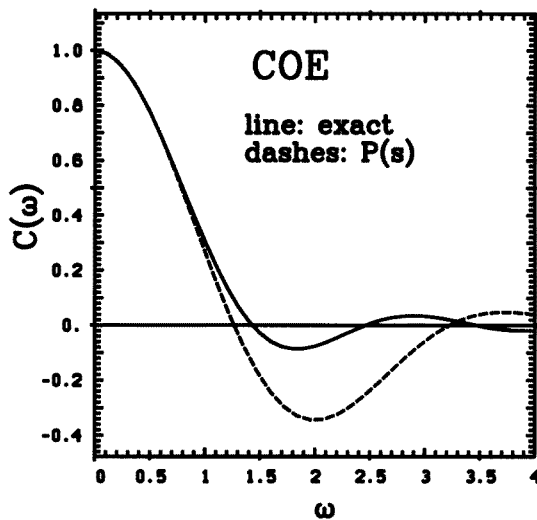


Figure 4. Comparison of the $N \rightarrow \infty$ results (full curve) and the results for spectra which only have the correct nearest-neighbour level spacing distribution but higher-order correlations are neglected (broken curve; $N = 40$). All results are for COE.

For this purpose we used the rejection method to generate a random ensemble of spectral sequences, with nearest-neighbour spacings which are distributed as $P_{\text{COE}}(s)$, disregarding all other correlations which are implied by the exact COE measure (65). In figure 4 we compare the expectation value of the autocorrelation function for this ensemble with the proper COE result. The difference between the two functions shows already at the positions of the first zero crossings, and the depths of the first minima. These differences are rather

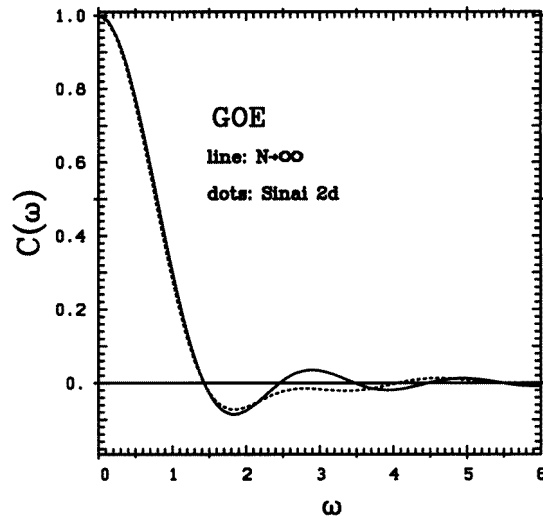


Figure 5. Autocorrelation function for the two-dimensional Sinai billiard. The spectrum is chopped into pieces with $N = 40$.

large, and establish the sensitivity of the autocorrelation function to correlations between levels which are further apart than the nearest-neighbours.

4.2. Application to spectra of physical systems

At this point we turn to the analysis of physical spectra, to check the extent of applicability of the semiclassical and the RMT results.

We used the spectra of Sinai billiards in two [19] and in three dimensions [20], for which we have the lowest 2591 and 6698 eigenvalues, respectively. We analysed the (unfolded) spectra using the two methods mentioned previously. In the first, the spectra were chopped into subintervals of length $N = 40$, and were centred around $E \approx 0$. We thus obtained numerical ensembles consisting of 64 and 167 intervals respectively. The average autocorrelation functions are compared with the corresponding metropolis data in figures 5 and 6. As the number of eigenvalues is quite small for the two-dimensional Sinai billiard, only the first minimum is reproduced correctly. However, the situation is improved when the larger spectrum for the three-dimensional billiard is analysed.

To use the entire spectral data in one run, we defined the correlation function as in (70) and applied it to the spectrum of the two-dimensional Sinai billiard, using all eigenvalues in one run. The result is given in figure 3 (dotted curve). The numerical values agree better with the MA runs for the regularized version. Both show nearly the same damping although the zeros are slightly shifted.

The conclusion we may draw from the comparison of the two methods, is that the regularized version has a built-in self-averaging mechanism. The energy integral represents an averaging over independent parts of the spectrum. At a certain value E only E_i which are close to E significantly contribute to the product (69).

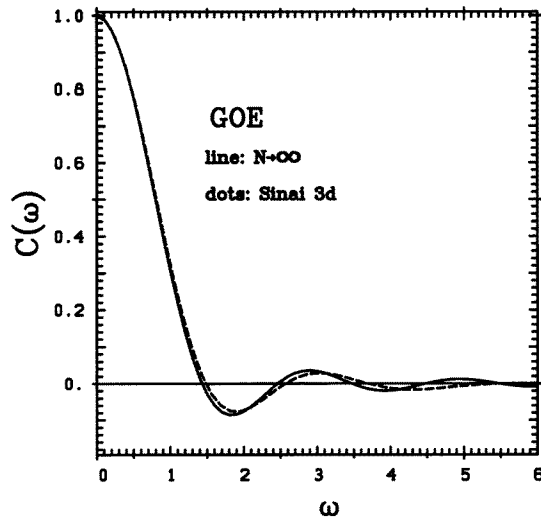


Figure 6. Same as in figure 5 but for three dimensions.

5. Conclusion

In this work we tried to emphasize the theoretical and practical advantages of the use of the autocorrelation function of spectral determinants, both as a practical statistical tool and as an alternative route to study the relationship between quantum chaos and RMT. To conclude, we would like to make a few further comments.

One of the most gratifying aspects of the present work was the fact that the correlations of the Riemann ζ on the critical line have much in common with the present work, and could be studied using rigorous mathematical tools [12]. This provides much more confidence in the *ad hoc* assumptions which were made in the development of the semiclassical theory.

Our work on the RMT expressions for the autocorrelation functions complements the previous results on the circular ensembles [8], and the known results for GUE [14]. It also provides the expressions for the GOE case, and for the ensembles which interpolate between GOE and GUE.

The semiclassical derivation of the autocorrelation function is new, and enables a close scrutiny of relevance of the classical ζ function to spectral statistics in the semiclassical limit. It is clear that both functions are derived from the same building blocks—as a matter of fact, their Fourier coefficients coincide up to the topological time which corresponds to half the Heisenberg time. This is in agreement with the recent observations of [7]. The semiclassical methods which were developed here can also be used for quantum chaotic problems for which the spectral statistics differ from the one expected for the standard Dyson ensembles. Such problems are commonly met in applications to mesoscopic systems.

Acknowledgments

This work was supported by the Minerva Center for Nonlinear Physics and the Israeli Science Foundation. The Minerva Foundation provided postdoctoral fellowships to SK and DK. We are grateful to H Primack and H Schanz for the spectra of the two- and three-dimensional Sinai billiards. We thank H Primack for performing some critical checks, and

for many comments and suggestions. We are indebted to F Haake, for reporting about his results prior to their publication, and to J Keating and Z Rudnik for stimulating discussions on the autocorrelation function of the Riemann ζ function.

Appendix. Grassmannian functional integration

Although the Grassmannian functional integrals (19) can be performed exactly, let us treat this expression as we usually do when one encounters an interacting theory: apply a Hubbard–Stratonovitch [17] transformation. If the resulting decoupled theory cannot be solved exactly, do a saddle-point approximation. Expansion around the saddle point then leads to a nonlinear sigma model theory which can possibly be integrated out. The advantage over the exact result turns out to be that the limit $N \rightarrow \infty$ can be done more easily and is exact. We may first write equation (19) more compactly (compare with [15, 14]):

$$\begin{aligned} \bar{C}_N(E, \omega) = & \int d\psi \exp\left(\frac{1}{2}i \sum_i \bar{\psi}_i \left(E + \frac{\omega}{2}\Lambda\right) \psi_i\right) \exp\left(-\frac{1}{16c} \text{Tr}\left(\sum_{i=1}^N \psi_i \otimes \bar{\psi}_i\right)^2\right) \\ & \times \exp\left(-\frac{\alpha^2}{16c} \text{Tr}\left(\sum_{i=1}^N \psi_i \otimes \bar{\psi}_i \tau_3\right)^2\right) \end{aligned} \quad (72)$$

where

$$\Lambda = \begin{pmatrix} 2x2 & 0 \\ 0 & -2x2 \end{pmatrix} \quad (73)$$

ensures that the ξ 's obtain a '+ ω ' and the η 's obtain a '- ω '.

$$\tau_3 = \begin{pmatrix} 1 & 0 \\ 0 & -1 \end{pmatrix} \quad (74)$$

has to be introduced due to the asymmetric part of the random matrices H_a . For compactness the vectors of anticommuting variables were introduced:

$$\psi_i = \begin{pmatrix} \xi_i \\ \xi_i^* \\ \eta_i \\ \eta_i^* \end{pmatrix} \quad \bar{\psi}_i = (\xi_i^*, -\xi_i, \eta_i^*, -\eta_i). \quad (75)$$

Now, one can decouple the interaction term by performing a Hubbard–Stratonovitch transformation [17], which introduces a functional integral over a matrix Q which has the same symmetries as the dyadic product $\psi_i \otimes \bar{\psi}_i$.

$$\begin{aligned} \bar{C}_N(E, \omega) = & \int d\psi dQ \exp\left(\frac{i}{2} \sum_{i=1}^N \bar{\psi}_i \left(E + \frac{\omega}{2}\Lambda\right) \psi_i\right) \\ & \times \exp\left(-4c \text{Tr} Q^2 + \text{Tr}\left[(a_1 Q + a_2 \tau_3 Q \tau_3) \sum_{i=1}^N \psi_i \otimes \bar{\psi}_i\right]\right) \end{aligned} \quad (76)$$

where $a_{1,2} = \frac{1}{2} \left(\sqrt{1+\alpha^2} - (-)^{1,2} \sqrt{1-\alpha^2}\right)$.

Next, the integral over the vector ψ can be performed, yielding

$$\int dQ \exp(-4c \text{Tr} Q^2) \det\left(a_1 Q + a_2 \tau_3 Q \tau_3 + \frac{i}{2} \left(E + \frac{\omega}{2}\Lambda\right)\right)^{N/2} \quad (77)$$

where we now put $c = \pi^2/4N$, explicitly.

Transforming $Q \rightarrow 2\pi/NQ$, one obtains:

$$\bar{C}_N(E, \omega) = \int dQ \exp \left[-\frac{N}{4} \text{Tr} Q^2 + \frac{N}{2} \text{Tr} \ln \left(\frac{N}{2\pi} (a_1 Q + a_2 \tau_3 Q \tau_3) + \frac{1}{2} i \left(E + \frac{\omega}{2} \Lambda \right) \right) \right]. \quad (78)$$

Variation with respect to Q yields $\text{Tr} \delta Q Q = \text{Tr} (a_1 Q + a_2 \tau_3 Q \tau_3)^{-1} (a_1 \delta Q + a_2 \tau_3 \delta Q \tau_3)$. To lowest order in the parameter α this saddle-point condition becomes $Q^2 = 1$. Expanding to lowest order in α and transforming $Q \rightarrow Q + \pi/Ni(E + \frac{\omega}{2} \Lambda)$ one obtains:

$$\begin{aligned} \bar{C}_N(E, \omega) = & \int dQ \exp(-N/4 \text{Tr} Q^2) \det Q^{N/2} \exp \left(\frac{\pi}{2} i \text{Tr} [(E + \frac{\omega}{2} \Lambda) Q] \right) \\ & \times \exp \left(\frac{N}{2} \alpha^2 \text{Tr} [Q \tau_3 Q \tau_3] \right) \end{aligned} \quad (79)$$

together with the symmetry restrictions of Q , $Q = \bar{Q}$ where $\bar{Q} = C Q^T C^T$ with $C = \begin{pmatrix} -i\tau_2 & 0 \\ 0 & i\tau_2 \end{pmatrix}$, with $\tau_2 = \begin{pmatrix} 0 & -i \\ i & 0 \end{pmatrix}$ and $Q = Q^+$ one obtains:

$$Q = \begin{pmatrix} q & A \\ A^+ & -q \end{pmatrix}. \quad (80)$$

with $A = \begin{pmatrix} a & b \\ b^* & -a^* \end{pmatrix}$ where $|a|^2 + |b|^2 + q^2 = 1$. In the saddle-point approximation \bar{C} is independent of E , since $\text{Tr} Q = 0$ for the above saddle-point manifold. Hence, the exponent in equation (79) is independent of E . For $N \rightarrow \infty$ this saddle-point approximation becomes exact.

A matrix Q with the above symmetries can be represented as,

$$Q = U^{-1} Q_c^0 U \quad (81)$$

with

$$U = V_C U_D \quad (82)$$

where

$$U_D = V_D^{-1} T_D^0 V_D \quad (83)$$

where

$$Q_c^0 = \begin{pmatrix} \cos \theta_C & i \sin \theta_C \tau_2 \\ i \sin \theta_C \tau_2 & -\cos \theta_C \end{pmatrix} \quad (84)$$

and

$$T_D^0 = \begin{pmatrix} \cos \theta_D/2 & i \sin \theta_D/2 \\ i \sin \theta_D/2 & \cos \theta_D/2 \end{pmatrix} \quad (85)$$

and

$$V_{C,D} = \begin{pmatrix} \exp(i\phi_{C,D} \tau_3) & 0 \\ 0 & 0 \end{pmatrix}. \quad (86)$$

and τ_i , $i = 1, 2, 3$ are the Pauli matrices. Such a representation was first given by Altland *et al* [15] to study the crossover between GOE and GUE within the supersymmetric nonlinear sigma model. Here, of course we need only the compact block of the representation given there.

In order to perform the functional integral in this representation, we have to find the corresponding integration measure. To this end we find

$$\text{Tr} dQ^2 = (d\theta_C d\theta_D d\phi_C d\phi_D) A (d\theta_C d\theta_D d\phi_C d\phi_D)^T$$

for this representation, and making use of $dQ = (\det A)^{1/2} d\theta_C d\theta_D d\phi_C d\phi_D$, we obtain finally:

$$dQ = 16 \cos \theta_C^2 |\sin \theta_C| |\sin \theta_D| d\theta_C d\theta_D d\phi_C d\phi_D. \quad (87)$$

As a result, we find for large N the normalized correlation function:

$$C_N(E, \omega) = C_N(\omega) = \int_0^1 d\lambda \lambda \frac{\sin(\pi\omega\lambda)}{\omega} \exp(t^2(\lambda^2 - 1)) / C_0(t^2) \quad (88)$$

where the normalization constant is given by

$$C_0(t^2) = \frac{2}{\pi} \int_0^1 d\lambda \lambda^2 \exp(t^2(\lambda^2 - 1)) \quad (89)$$

and $t^2 = 4N\alpha^2$.

Integral (88) can be expressed in terms of the error function with complex argument:

$$C_N(\omega) = \frac{\pi^{3/2} \frac{1}{t} \exp\left(\frac{\pi^2 \omega^2}{4t^2}\right) \Im[\text{erfc}\left(\frac{\pi\omega}{2t} + it\right)] - 2e^{t^2} \frac{\sin(\pi\omega)}{\omega}}{\pi^{3/2} \frac{1}{t} \Im[\text{erfc}(it)] - 2e^{t^2} \pi} \quad (90)$$

where $\text{erfc}(z)$ is the complementary error function.

References

- [1] Bohigias O, Giannoni M J and Schmit C 1984 *Phys. Rev. Lett.* **52** 1
- [2] Smilansky U 1991 *Proc. 1989 Les Houches Summer School Chaos and Quantum Physics* ed M J Giannoni and J Zinn-Justin 371
- [3] Berry M V 1985 *Proc. R. Soc. A* **400** 229
- [4] Andreev A V and Altshuler B L 1995 *Phys. Rev. Lett.* **75** 902
- [5] Agam O, Altshuler B L and Andreev A V 1995 *Phys. Rev. Lett.* **75** 4389
- [6] Muzykantskii B A and Khmel'nitskii D E 1995 *JETP Lett.* **62** 76
- [7] Bogomolny E B and Keating J 1996 *Phys. Rev. Lett.* **77** 1472
- [8] Haake F, Kuš M, Sommers H-J, Schomerus H and Zyczkowski K 1996 *J. Phys. A: Math. Gen.* **29** 3641
- [9] Bogomolny E B 1992 *Nonlinearity* **5** 805
- [10] Doron E and Smilansky U 1992 *Nonlinearity* **5** 1055
- [11] Keating J and Berry M V 1992 *Proc. R. Soc. A* **437** 151
- [12] Cheung J Y and Keating J 1997 Correlations in ζ functions *Preprint*
- [13] Dyson F J 1962 *J. Math. Phys.* **3** 140
- [14] Andreev A V and Simons B D 1995 *Phys. Rev. Lett.* **75** 2304
- [15] Altland A, Iida S and Efetov K B 1993 *J. Phys. A: Math. Gen.* **26** 3545
- [16] Efetov K B 1983 *Adv. Phys.* **32** 53
- [17] Stratonovich R L 1958 *Sov. Phys.-Doklady* **2** 416
Hubbard J 1959 *Phys. Lett.* **3** 77
- [18] Metropolis N, Rosenbluth A, Rosenbluth M, Teller A and Teller M 1953 *J. Chem. Phys.* **21** 1081
- [19] Schanz H and Smilansky U 1995 *Chaos, Solitons and Fractals* **5** 1289
- [20] Primack H and Smilansky U 1995 *Phys. Rev. Lett.* **74** 4831
- [21] Plemelj J 1909 *Monat. Math. Phys.* **15** 93
- [22] Hannay H J and Ozorio de Almeida A M 1987 *J. Phys. A: Math. Gen.* **17** 3429